

Exploring sub-GeV Dark Matter Physics with Cosmic Ray and Future Telescopes

Guansen Wang,^{1,2} Bing-Yu Su,^{1,2,*} Lei Zu,^{3,†} and Lei Feng^{1,2,4,‡}

¹Key Laboratory of Dark Matter and Space Astronomy,

Purple Mountain Observatory, Chinese Academy of Sciences, Nanjing 210023, China

²School of Astronomy and Space Science, University of Science and Technology of China, Hefei 230026, China

³National Centre for Nuclear Research, ul. Pasteura 7, 02-093 Warsaw, Poland

⁴Joint Center for Particle, Nuclear Physics and Cosmology,

Nanjing University – Purple Mountain Observatory, Nanjing 210093, China

If sub-GeV Dark matter(DM) annihilates to the charged particles such as e^+e^- , $\mu^+\mu^-$, or $\pi^+\pi^-$, it generates an additional source of electrons and positrons in the cosmic ray (CR) population within our Milky Way. During propagation, these secondary electrons and positrons undergo reacceleration processes, boosting their energies to the GeV scale. Observatories like AMS-02 can detect these high-energy particles, enabling constraints on the properties of sub-GeV DM. By analyzing AMS-02 electron and positron data, the 95% upper limits on the DM annihilation cross-section have been established in the range of 10^{-28} to 10^{-27} $\text{cm}^3 \text{s}^{-1}$, corresponding to DM masses ranging from 100 MeV to 1 GeV. Meanwhile, MeV telescopes will provide complementary constraints on DM properties by detecting photon emissions from such annihilation processes. Notably, the sensitivity of future MeV gamma-ray observatories is projected to approach or match the constraints derived from CR data.

I. INTRODUCTION

Over the past decades, dark matter (DM) has remained one of the most pressing mysteries in astrophysics and cosmology. While extensive evidence for its existence has been gathered from galactic rotation curves, gravitational lensing, and observations of the cosmic microwave background (CMB), the precise nature and interaction mechanisms of DM remain elusive. Historically, much of the research has focused on DM candidates in the GeV–TeV mass range, commonly referred to as weakly interacting massive particles (WIMPs). These particles naturally explain the observed DM relic density through the thermal freeze-out mechanism [1–7]. Despite decades of dedicated effort, no conclusive evidence for WIMPs has been found. A wide range of experiments designed to probe WIMP interactions has yielded null results. Direct detection experiments such as XENONnT, LUX, and PandaX [8–13] have excluded significant portions of the parameter space for DM-baryon and DM-electron interactions for WIMPs with masses above the GeV scale. Similarly, indirect searches through cosmic ray (CR) and γ -ray observations such as AMS-02 and Fermi-LAT have placed strong constraints on DM annihilation. These results have shifted the attention of researchers toward exploring alternative DM mass ranges, particularly in the MeV (sub-GeV) scale [14–20]. Such low-mass DM candidates present new opportunities and challenges for detection, potentially offering critical insights into the nature of DM.

However, both traditional direct and indirect detection methods for DM face significant challenges when probing

the sub-GeV mass range. Direct detection experiments rely on the nuclear recoil mechanism, which becomes less sensitive as the DM mass drops significantly below the mass of the target nuclei, typically on the GeV scale. Consequently, the signals from sub-GeV DM are greatly suppressed. On the other hand, indirect detection methods also face challenges in this mass range due to limitations in detecting sub-GeV photons. MeV astrophysics, in particular, has historically suffered from a lack of observations and understanding, often referred to as the “MeV gap”. This energy range lies between the well-explored keV scale of X-ray astronomy and the GeV–TeV range of γ -ray astrophysics. The absence of sensitive instruments capable of studying MeV-scale phenomena has impeded progress in detecting photon signals from sub-GeV DM annihilation or decay. Several strategies have been proposed to address this issue, including the CR boosted DM in direct detection [21–32] and CR reacceleration in CR detection [19, 20]. Reacceleration effect describes how CRs interact with magnetic fields and gas in the galaxy, influencing their propagation paths and energy distributions. It will boost the sub-GeV electrons to GeV scale, making it detectable by the CR experiments like AMS-02.

In this work, we utilize the CR reacceleration effect to calculate the propagation of secondary electrons and positrons produced from DM annihilation. Following previous research, we explore additional annihilation channels and account for uncertainties in CR propagation parameters. Specifically, we consider channels such as e^+e^- , $\mu^+\mu^-$, 4 electrons, 4 muons and $\pi^+\pi^-$ channels. We also investigate the potential impact of uncertain CR propagation parameters. By analyzing AMS-02 electron and positron data, we derive constraints on the DM annihilation cross-section, which range from 10^{-28} to 10^{-27} $\text{cm}^3 \text{s}^{-1}$, corresponding to the DM mass from 100 MeV to 1 GeV. These bounds are comparable to those obtained

* bysu@pmo.ac.cn

† Lei.Zu@ncbj.gov.pl

‡ fenglei@pmo.ac.cn

from CMB data and are significantly more stringent than limits derived from Voyager observations [19, 33].

Additionally, we calculate the MeV photon flux resulting from final state radiation or the decay of annihilation products. Under optimistic estimations, DM-rich regions are capable of producing sufficient MeV photons to be detectable by upcoming MeV gamma-ray telescopes, such as AMEGO [34], AMEGO-X [35], MEGA [36], GRIPS [37], e-Astrogam [38] and Very Large Area gamma-ray Space Telescope (VLAST) [39]. This indicates that the high sensitivity MeV telescope in the future are crucial for exploring the physics of sub-GeV DM. The detection of MeV photons complements CR observations, as it provides an independent and direct probe of DM annihilation or decay processes. While CR experiments like AMS-02 are sensitive to the charged particle products of DM interactions, MeV gamma-ray telescopes can capture the secondary electromagnetic signatures, offering a more comprehensive picture of DM behavior.

This work is organized as follows: In Sec. II, we analyse the electrons and positrons spectrum from DM annihilation, and present the properties of the Milky Way. Then we calculate the background CR spectrum in Sec. III, followed by a summary of the results related to CRs in Sec. IV. Additionally, in Sec. V, we calculate the gamma-ray radiation produced by DM annihilation. Finally, we conclude in Sec. VI.

II. MODELING SUB-GEV DM ANNIHILATION AND CR PROPAGATION

In this work, we investigate sub-GeV DM annihilation in the Milky Way by utilizing AMS-02 electron and positron data, incorporating the effects of reacceleration. To describe the DM density profile in our Milky Way, we use NFW profile [40]

$$\rho = \frac{\rho_s}{r/r_s(1+r/r_s)^2}, \quad (1)$$

with a local density $\rho_0 = 0.3 \text{ GeV cm}^{-3}$ [41], where ρ_s and r_s are the characteristic density and radius. We consider sub-GeV DM particles annihilating into various final states, including e^+e^- , $\mu^+\mu^-$, 4 electrons/positrons, 4 muons and $\pi^+\pi^-$. Final states involving muons or pions subsequently decay, producing secondary electrons/positrons and the photons that contribute to the observed CR and MeV photon spectrum. These processes has been studied in previous work [42] (referred to as ‘‘PPPC4’’), where the authors simulated the full spectrum using the Pythia package [43]. For the specific case of electrons produced from the pion annihilation channel, we employ the HAZMA code [44], a publicly available tool specialized in modeling sub-GeV DM annihilation and decay.

Unlike photons, the propagation of charged CRs is significantly influenced by the local environment, including magnetic fields, interstellar gas, and turbulence. These

factors can alter the energy distributions of charged particles, leading to effects such as diffusion, reacceleration, and energy losses. To calculate the propagation of these secondary electrons and positrons, we use the public code LikeDM [45], which is based on a Green function approach derived from numerical tables provided by GALPROP [46]. LikeDM has been validated to produce results consistent with GALPROP while offering significantly improved computational efficiency. The propagation parameters, including the diffusion coefficient D_0 , the Alfvénic speed v_A (which characterizes the reacceleration effect) and the half-height of the propagation cylinder z_h are determined by fitting to the Boron-to-Carbon ratio data and the Fermi diffuse γ -ray emission [47]. To account for uncertainties in CR propagation, we adopt a set of propagation parameters, listed in Table I, which allows us to evaluate the robustness of our results.

	D_0 ($28 \text{ cm}^2 \text{ s}^{-1}$)	z_h (kpc)	v_A (km s^{-1})	δ
Prop. 1	2.7	2	35.0	0.33
Prop. 2	5.3	4	33.5	0.33
Prop. 3	7.1	6	31.1	0.33
Prop. 4	8.3	8	29.5	0.33
Prop. 5	9.4	10	28.6	0.33
Prop. 6	10.0	15	26.3	0.33

TABLE I: Propagation parameters with z_h varying from 2 kpc to 15 kpc. Suppose a homogeneous spatial diffusion coefficient $D_{xx} = D_0\beta(E/4 \text{ GeV})^\delta$, where β is the Lorentz factor, D_0 is a coefficient, and $\delta = 0.33$ reflects the Kolmogorov-type interstellar medium turbulence. The Alfvénic speed v_A characterizes the reacceleration effect.

III. CR BACKGROUND

To detect the signal of DM annihilation products in CR, it is essential to accurately model the astrophysical CR background. This background consists of primary electrons from sources such as supernova remnants and pulsars, as well as secondary electrons and positrons produced by inelastic collisions between CR nuclei and the interstellar medium.

The injection spectrum of primary electrons is modeled using a three-segment broken power-law with an exponential cutoff [20]. The spectrum is given by:

$$\Phi_{e^-} = A_{e^-} E^{-\nu_1^-} [1 + (E/E_{br1}^-)^3]^{(\nu_1^- - \nu_2^-)/3} \times [1 + (E/E_{br2}^-)^3]^{(\nu_2^- - \nu_3^-)/3} \exp(-E/E_c^-). \quad (2)$$

where A_{e^-} is the normalized factor and $\nu_{1,2,3}^-$ are the power-law indices for the three segments. The first spectral break (E_{br1}^-), at a few GeV, accounts for low-energy

data, while the second break ($E_{br2}^{e^-}$), at several tens of GeV, captures the observed spectral hardening. The exponential cutoff ($E_c^{e^-}$) is introduced to fit high-energy data, though its effect on the energy range considered here is minimal [1, 48, 49].

Secondary electrons and positrons are produced by inelastic collisions between CR nuclei and the interstellar medium. The spectrum of secondary positron resulting from pp collisions is calculated by GALPROP. During the fitting process, the flux is scaled by a constant factor to accommodate potential uncertainties in the theoretical predictions [50].

Additionally, a pulsar-like component is incorporated into the model. The injection spectrum of electrons and positrons from pulsars follows an exponential cut-off power-law:

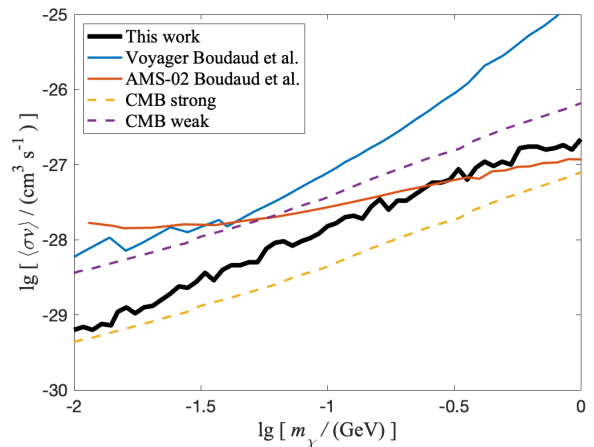
$$\Phi_{\text{psr}} = A_{\text{psr}} E^{-\nu^{\text{psr}}} \exp(-E/E_c^{\text{psr}}), \quad (3)$$

where E_c^{psr} is the cutoff for the pulsar component and ν^{psr} , A_{psr} represent the power index and normalized parameter. The spatial distribution of pulsars is assumed to follow that of primary CR sources [46]. After the astrophysical background is well-modeled, the residual flux (after subtracting the background) can be analyzed for potential signals of DM annihilation.

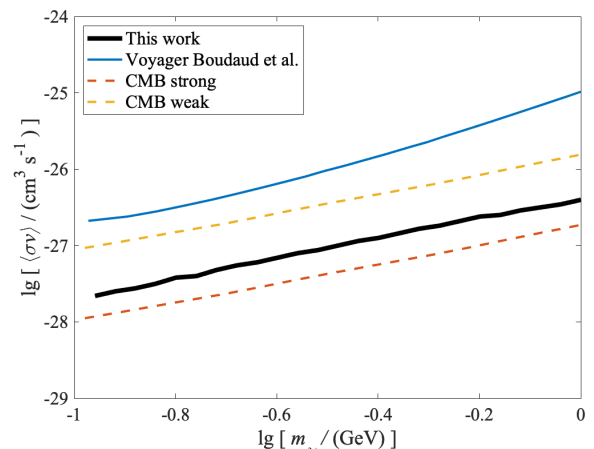
IV. RESULTS FROM CRS

With the injection spectra of different source components, we can calculate the corresponding propagated spectra and compare them with observational data. Assuming the DM annihilates to e^+e^- , $\mu^+\mu^-$ or $\pi^+\pi^-$ within the Milky Way halo, we employ a maximum likelihood fitting approach to search for the DM component. The CR data we used includes the AMS-02 positron fraction and the total electron plus positron flux [51, 52]. We calculate the χ^2 for each DM parameter and find the minimum χ^2 as the best-fit χ_0^2 . Then, by setting $\Delta\chi^2 = \chi^2 - \chi_0^2 > 2.71$, we derive the 2σ upper limits of the DM annihilation cross section.

First, we use Prop. 2 from Table I as the benchmark propagation model to illustrate the constraints. If DM annihilates into e^+e^- or $\mu^+\mu^-$, we present the 95% upper limits on the annihilation cross-section in Fig. 1. For DM masses ranging from 100 MeV to 1 GeV, our derived limits on the annihilation cross-section lie between 10^{-28} and $10^{-27} \text{ cm}^3 \text{ s}^{-1}$, which are comparable to the results from CMB [53, 54] and are more stringent than those derived from Voyager data [19] for more than an order. The annihilation of DM into charged particles and photons is constrained by observations of the CMB, which influence the ionization fraction and modify CMB anisotropies. Previous studies indicate that the limit is set as $f_{\text{eff}}\langle\sigma v\rangle/2m_\chi < 4.1 \times 10^{-28} \text{ cm}^3 \text{ s}^{-1} \text{ GeV}^{-1}$, where f_{eff} is the effective efficiency factor. In this analysis, we use $f_{\text{eff}} = 0.08$ for a conservative limit and



(a) Electron



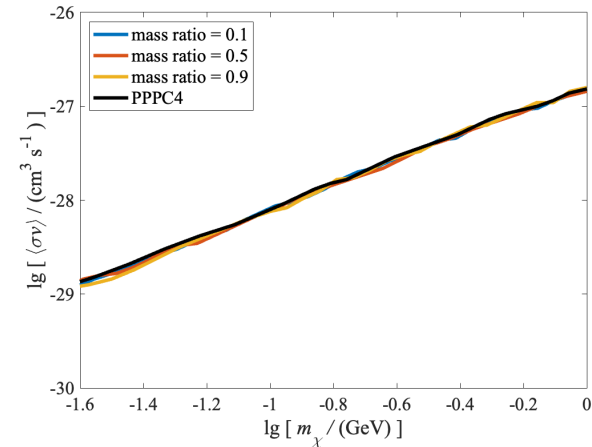
(b) Muon

FIG. 1: The upper limits of DM annihilation cross section $\langle\sigma v\rangle$. The results of e^+e^- and $\mu^+\mu^-$ are shown in Figs. 1a and 1b.

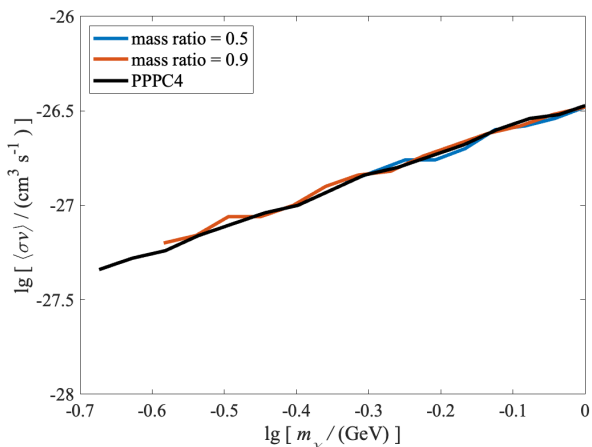
$f_{\text{eff}} = 1$ for a progressive limit, leading to the constraints $\langle\sigma v\rangle_{\bar{f}f}/(2m_\chi) \leq 5.1 \times 10^{-27} \text{ cm}^3 \text{ s}^{-1} \text{ GeV}^{-1}$ and $\langle\sigma v\rangle_{\bar{f}f}/(2m_\chi) \leq 4.1 \times 10^{-28} \text{ cm}^3 \text{ s}^{-1} \text{ GeV}^{-1}$ [53, 54].

Additionally, if DM annihilates into four electrons or four muons via light mediators, this study provides new constraints on these less explored annihilation channels, probing different aspects of DM interactions (see Fig. 2). To further investigate the impact of the intermediate particle mass on the results, we examined scenarios where the intermediate particle masses are set to 0.1, 0.5, and 0.9 times the DM mass. The results were compared with those from PPC4, and they were found to be nearly identical. This consistency suggests that the intermediate particle mass, within the considered range, has a negligible effect on the final outcomes. The pion results are also shown in Fig. 3.

To assess the robustness of our results with respect to the choice of propagation parameters, we examine the un-



(a) 4 electrons



(b) 4 muons

FIG. 2: The upper limits of DM annihilation cross section $\langle\sigma v\rangle$. The results of 4 electrons are shown in Fig. 2a, along with 4 muons in Fig. 2b.

certainties in CR propagation by employing six distinct propagation models (Props. 1 to 6) listed in Table I for the e^+e^- scenario. These results are illustrated in Fig. 4. Our analysis reveals that the uncertainty introduced by CR propagation stays within one order of magnitude across the models. Notably, Prop. 2, which was used to derive the constraints discussed earlier, emerges as the most conservative model among the set. This demonstrates the stability of our findings under varying propagation assumptions.

V. RESULTS FROM PHOTONS

When the DM annihilates to some charged particles, final state radiation of photons is inevitably produced. These photons provide complementary information to the study of DM annihilation. Unlike charged particles,

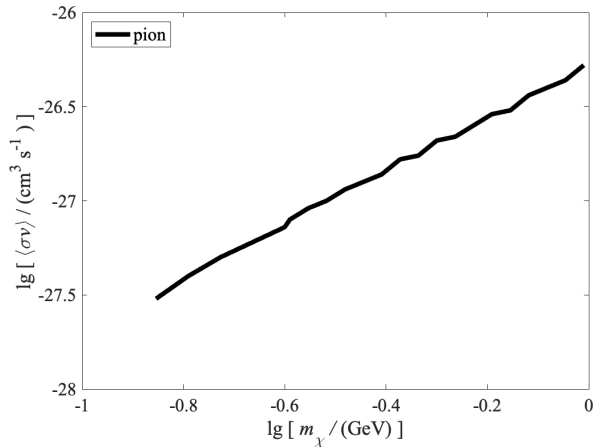


FIG. 3: The upper limits of DM annihilation cross section $\langle\sigma v\rangle$ of pion channel.

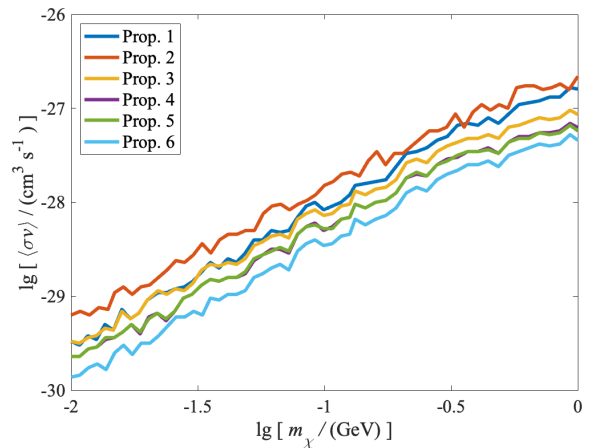


FIG. 4: The upper limits of DM annihilation cross section $\langle\sigma v\rangle$ with different propagation parameters. The results of e^+e^- channel.

photons are not affected by interstellar magnetic fields and propagate directly, offering a clearer signature of the annihilation process. By combining photon signals with cosmic ray observations, a multi-messenger approach can be employed to enhance the detection capability and scientific understanding of DM annihilation.

In this section, we investigate photon emissions resulting from DM annihilation in the Galactic Center (GC), complementing our study of DM annihilation processes in the broader Milky Way. The GC is a region of particular interest due to its high predicted dark matter density, which makes it a prime target for detecting potential DM annihilation photon signals. The photons from the final state radiation primarily occurs at the sub-GeV scale. While no high-sensitivity telescopes currently operate in this energy range, several proposed missions, such as the All-sky Medium Energy Gamma-ray Observatory

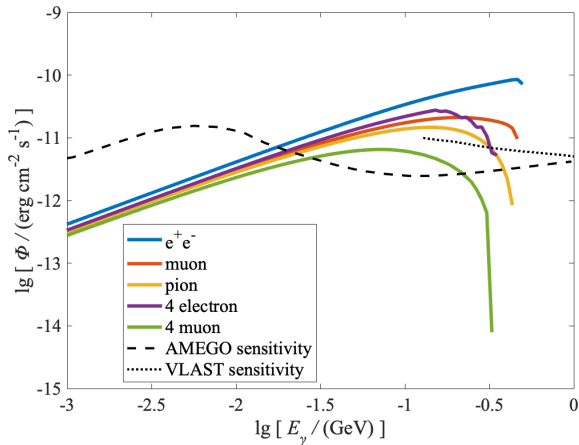


FIG. 5: The energy flux of gamma-ray photons resulting from the final state radiation of DM in the Galactic halo across different annihilation channels is depicted. The black dashed line represents the sensitivity of AMEGO.

(AMEGO)[44] and Very Large Area gamma-ray Space Telescope(VLAST)[39], are expected to be launched in the near future, significantly enhancing our understanding of sub-GeV astrophysical phenomena.

In this analysis, we adopt the same DM density profile as used in the CR study. This profile yields a J-factor of $2.503 \times 10^{22} \text{ GeV}^2 \text{ cm}^{-5}$ within ± 5 degrees [45], which quantifies the line-of-sight integral of the squared DM density and is critical for calculating the expected annihilation flux. We focus on a DM mass of 500 MeV and compute the final state radiation photon fluxes for various annihilation channels. The results are presented as solid lines in the Fig. 5, with different colors corresponding to different final states.

The predicted photon fluxes are compared with the sensitivity curves of upcoming gamma-ray telescopes including the AMEGO and VLAST, represented as dashed and dotted lines in the figure¹. The expected photon flux from DM annihilation has been found to reach the sensitivity thresholds of future gamma-ray telescopes. The results demonstrate that AMEGO and VLAST will play a crucial role in constraining the properties of sub GeV DM and could potentially uncover definitive evidence of

DM annihilation in the Milky Way.

VI. CONCLUSION

The search for DM annihilation signals through CRs and future MeV gamma-ray telescopes represents a powerful and complementary approach to unraveling the mysteries of DM. By analyzing CR data from experiments like AMS-02, we have constrained the sub-GeV DM annihilation cross-section in the range of 10^{-28} to $10^{-27} \text{ cm}^3 \text{ s}^{-1}$, corresponding to DM masses ranging from 100 MeV to 1 GeV. However, the limitations of CR detection due to the uncertainty of the astrophysical backgrounds and propagation process, highlight the need for alternative detection methods.

Future MeV gamma-ray telescopes, such as AMEGO and VLAST, offer a promising avenue to overcome these challenges. These instruments are designed to bridge the "MeV gap," providing unprecedented sensitivity to photon signals from DM annihilation. Our analysis demonstrates that the expected photon fluxes from DM-rich regions, such as the Galactic Center, could reach the detection thresholds of these telescopes.

The combination of CR and MeV gamma-ray observations enables a multi-messenger approach to DM detection. While CRs provide insights into charged particle products of DM annihilation, MeV photons offer a direct and complementary probe of the annihilation process, free from the confounding effects of interstellar magnetic fields. Together, these methods enhance our ability to disentangle DM signals from astrophysical backgrounds and constrain DM properties with greater precision.

ACKNOWLEDGMENTS

This work is supported by the National Key R&D Program of China (Grant No. 2022YFF0503304), the National Natural Science Foundation of China (Grant Nos. 12373002, 12220101003, and 11773075), and the Youth Innovation Promotion Association of Chinese Academy of Sciences (Grant No. 2016288). LZ is supported by the NAWA Ulam fellowship (No. BPN/ULM/2023/1/00107/U/00001) and the National Science Centre, Poland (research grant No. 2021/42/E/ST2/00031).

¹ Although the sensitivities for point sources and extended sources are in principle different, they are expected to be of the same order of magnitude (see, e.g., [55]). For simplicity, we show the point source sensitivity here as a representative benchmark.

- [1] L. Feng, R. Z. Yang, H. N. He, T. K. Dong, Y. Z. Fan and J. Chang, Phys. Lett. B **728** (2014), 250-255 [arXiv:1303.0530 [astro-ph.HE]].
- [2] M. Pospelov, A. Ritz and M. B. Voloshin, Phys. Lett. B **662** (2008), 53-61 [arXiv:0711.4866 [hep-ph]].
- [3] S. Alekhin, W. Altmannshofer, T. Asaka, B. Batell, F. Bezrukov, K. Bondarenko, A. Boyarsky, K. Y. Choi, C. Corral and N. Craig, *et al.* Rept. Prog. Phys. **79** (2016)

- no.12, 124201 [arXiv:1504.04855 [hep-ph]].
- [4] L. Roszkowski, E. M. Sessolo and S. Trojanowski, Rept. Prog. Phys. **81** (2018) no.6, 066201 [arXiv:1707.06277 [hep-ph]].
- [5] T. R. Slatyer, N. Padmanabhan and D. P. Finkbeiner, Phys. Rev. D **80** (2009), 043526 [arXiv:0906.1197 [astro-ph.CO]].
- [6] E. Aprile *et al.* [XENON], JCAP **11** (2020), 031 [arXiv:2007.08796 [physics.ins-det]].
- [7] J. M. Gaskins, Contemp. Phys. **57** (2016) no.4, 496-525 [arXiv:1604.00014 [astro-ph.HE]].
- [8] E. Aprile *et al.* [XENON], Phys. Rev. Lett. **131** (2023) no.4, 041003 doi:10.1103/PhysRevLett.131.041003 [arXiv:2303.14729 [hep-ex]].
- [9] E. Aprile *et al.* [XENON], Phys. Rev. Lett. **121** (2018) no.11, 111302 doi:10.1103/PhysRevLett.121.111302 [arXiv:1805.12562 [astro-ph.CO]].
- [10] D. S. Akerib *et al.* [LUX], Phys. Rev. Lett. **118** (2017) no.2, 021303 doi:10.1103/PhysRevLett.118.021303 [arXiv:1608.07648 [astro-ph.CO]].
- [11] D. S. Akerib *et al.* [LUX], Phys. Rev. Lett. **112** (2014), 091303 doi:10.1103/PhysRevLett.112.091303 [arXiv:1310.8214 [astro-ph.CO]].
- [12] X. Cui *et al.* [PandaX-II], Phys. Rev. Lett. **119** (2017) no.18, 181302 doi:10.1103/PhysRevLett.119.181302 [arXiv:1708.06917 [astro-ph.CO]].
- [13] A. Tan *et al.* [PandaX-II], Phys. Rev. Lett. **117** (2016) no.12, 121303 doi:10.1103/PhysRevLett.117.121303 [arXiv:1607.07400 [hep-ex]].
- [14] G. S. Wang, Z. F. Chen, L. Zu, H. Gong, L. Feng and Y. Z. Fan, JCAP **05** (2024), 129 [arXiv:2303.14117 [astro-ph.HE]].
- [15] B. Y. Su, X. Pan, G. S. Wang, L. Zu, Y. Yang and L. Feng, Eur. Phys. J. C **84** (2024) no.6, 606 [erratum: Eur. Phys. J. C **84** (2024) no.8, 768] [arXiv:2403.04988 [astro-ph.HE]].
- [16] A. H. G. Peter, [arXiv:1201.3942 [astro-ph.CO]].
- [17] G. Bertone and D. Hooper, Rev. Mod. Phys. **90** (2018) no.4, 045002 [arXiv:1605.04909 [astro-ph.CO]].
- [18] K. Arun, S. B. Gudennavar and C. Sivaram, Adv. Space Res. **60** (2017), 166-186 [arXiv:1704.06155 [physics.gen-ph]].
- [19] M. Boudaud, J. Lavalle and P. Salati, Phys. Rev. Lett. **119** (2017) no.2, 021103 [arXiv:1612.07698 [astro-ph.HE]].
- [20] L. Zu, X. Pan, L. Feng, Q. Yuan and Y. Z. Fan, JCAP **08** (2022) no.08, 028 [arXiv:2104.03340 [hep-ph]].
- [21] S. Tulin and H. B. Yu, Phys. Rept. **730** (2018), 1-57 [arXiv:1705.02358 [hep-ph]].
- [22] L. Bergström, Rept. Prog. Phys. **63** (2000), 793 [arXiv:hep-ph/0002126 [hep-ph]].
- [23] G. Arcadi, M. Dutra, P. Ghosh, M. Lindner, Y. Mambrini, M. Pierre, S. Profumo and F. S. Queiroz, Eur. Phys. J. C **78** (2018) no.3, 203 [arXiv:1703.07364 [hep-ph]].
- [24] S. Navas *et al.* [Particle Data Group], Phys. Rev. D **110** (2024) no.3, 030001
- [25] M. Cirelli, Pramana **79** (2012), 1021-1043 [arXiv:1202.1454 [hep-ph]].
- [26] R. K. Leane, [arXiv:2006.00513 [hep-ph]].
- [27] L. Bergstrom, Annalen Phys. **524** (2012), 479-496 [arXiv:1205.4882 [astro-ph.HE]].
- [28] X. J. Bi, P. F. Yin and Q. Yuan, Front. Phys. (Beijing) **8** (2013), 794-827 [arXiv:1409.4590 [hep-ph]].
- [29] A. Kar, B. Mukhopadhyaya, S. Tingay, B. McKinley, M. Haverkorn, S. McSweeney, N. Hurley-Walker, S. Mitra and T. R. Choudhury, Phys. Dark Univ. **30**, 100689 (2020) [arXiv:2005.11962 [astro-ph.HE]].
- [30] Z. Chen, Y. L. S. Tsai and Q. Yuan, JCAP **09** (2021), 025 [arXiv:2105.00776 [astro-ph.HE]].
- [31] J. A. R. Cembranos, Á. De La Cruz-Dombriz, V. Gammaldi and M. Méndez-Isla, Phys. Dark Univ. **27** (2020), 100448 [arXiv:1905.11154 [hep-ph]].
- [32] W. Q. Guo, Y. Li, X. Huang, Y. Z. Ma, G. Beck, Y. Chandola and F. Huang, [arXiv:2209.15590 [astro-ph.HE]].
- [33] E. C. Stone, A. C. Cummings, F. B. McDonald, B. C. Heikkila, N. Lal and W. R. Webber, Science **341** (2013) no.6142, 1236408
- [34] R. Caputo *et al.* [AMEGO], [arXiv:1907.07558 [astro-ph.IM]].
- [35] H. Fleischhack, PoS **ICRC2021** (2021), 649 [arXiv:2108.02860 [astro-ph.IM]].
- [36] Andritschke, R., Zoglauer, A., Kanbach, G. et al., Exp Astron **20**, 395-403 (2005).
- [37] J. Greiner, AIP Conf. Proc. **1000** (2008) no.1, 620 [arXiv:0808.0267 [astro-ph]].
- [38] A. De Angelis *et al.* [e-ASTROGAM], JHEAp **19** (2018), 1-106 [arXiv:1711.01265 [astro-ph.HE]].
- [39] Y. Z. Fan, et al., Acta Astronomica Sinica **63**, 27 (2022).
- [40] J. F. Navarro, C. S. Frenk and S. D. M. White, Astrophys. J. **490** (1997), 493-508 [arXiv:astro-ph/9611107 [astro-ph]].
- [41] G. Bertone, M. Cirelli, A. Strumia and M. Taoso, JCAP **03** (2009), 009 [arXiv:0811.3744 [astro-ph]].
- [42] M. Cirelli, G. Corcella, A. Hektor, G. Hutsi, M. Kadastik, P. Panci, M. Raidal, F. Sala and A. Strumia, JCAP **03** (2011), 051 [erratum: JCAP **10** (2012), E01] [arXiv:1012.4515 [hep-ph]].
- [43] T. Sjostrand, S. Mrenna and P. Z. Skands, Comput. Phys. Commun. **178** (2008), 852-867 [arXiv:0710.3820 [hep-ph]].
- [44] A. Coogan, L. Morrison and S. Profumo, JCAP **01** (2020), 056 [arXiv:1907.11846 [hep-ph]].
- [45] X. Huang, Y. L. S. Tsai and Q. Yuan, Comput. Phys. Commun. **213** (2017), 252-263 [arXiv:1603.07119 [hep-ph]].
- [46] A. W. Strong and I. V. Moskalenko, Astrophys. J. **509** (1998), 212-228 [arXiv:astro-ph/9807150 [astro-ph]].
- [47] L. Bergstrom, T. Bringmann, I. Cholis, D. Hooper and C. Weniger, Phys. Rev. Lett. **111** (2013), 171101 [arXiv:1306.3983 [astro-ph.HE]].
- [48] Q. Yuan and X. J. Bi, Phys. Lett. B **727** (2013), 1-7 [arXiv:1304.2687 [astro-ph.HE]].
- [49] X. Li, Z. Q. Shen, B. Q. Lu, T. K. Dong, Y. Z. Fan, L. Feng, S. M. Liu and J. Chang, Phys. Lett. B **749** (2015), 267-271 [arXiv:1412.1550 [astro-ph.HE]].
- [50] S. J. Lin, Q. Yuan and X. J. Bi, Phys. Rev. D **91** (2015) no.6, 063508 [arXiv:1409.6248 [astro-ph.HE]].
- [51] M. Aguilar *et al.* [AMS], Phys. Rev. Lett. **110** (2013), 141102
- [52] M. Aguilar *et al.* [AMS], Phys. Rev. Lett. **113** (2014), 221102
- [53] T. R. Slatyer, Phys. Rev. D **93** (2016) no.2, 023527 [arXiv:1506.03811 [hep-ph]].
- [54] R. K. Leane, T. R. Slatyer, J. F. Beacom and K. C. Y. Ng, Phys. Rev. D **98** (2018) no.2, 023016 [arXiv:1805.10305 [hep-ph]].

[55] M. Negro, H. Fleischhack, A. Zoglauer, S. Digel and M. Ajello, *Astrophys. J.* **927** (2022) no.2, 225

doi:10.3847/1538-4357/ac5326 [arXiv:2111.10362 [astro-ph.HE]].